FAULT RESPONSE IN MICROGRIDS WITH FUEL CELLS

Marija Čuljak[1,2], Ivan Grcić[1], Hrvoje Pandžić[1]* , Juraj Havelka[1]

[1]*University of Zagreb Faculty of Electrical Engineering and Computing, Zagreb, Croatia*
[2]*KONČAR - Electrical Engineering Institute Ltd., Zagreb, Croatia*
*E-mail: hrvoje.pandzic@fer.hr

Keywords: FUEL CELL, FAULT ANALYSIS, MICROGRID

Abstract

Renewable energy sources (RES) are increasingly integrated into the power system to reduce the emission of greenhouse gases into the atmosphere. These sources are often grouped into entities, called microgrids, that can operate independently of the utility grid. Since the production of RES is variable and intermittent, there is a need for controllable, flexible and reliable power assets with zero emissions that can cancel out the RES output power fluctuations. Fuel cells fulfil these conditions and are an attractive complement to the RES-based microgrids. To address the behaviour of fuel cells inside the microgrid environment under fault behaviour, this work provides an analysis of its fault response. In doing so, the fuel cell is subjected to various types of faults in both standalone and microgrid operation.

1 Introduction

Renewable energy sources (RES) primarily use solar and wind energy to generate electricity. These sources displace conventional power generation from fossil fuels and reduce greenhouse gas emissions [1]. The RES with large capacity are usually grouped together (e.g. wind farms) and have a severe individual impact on power system operation, see e.g. [2]. In contrast, the RES of lower power are installed close to consumers, allowing the formation of microgrids – groups of local power sources and loads that can operate independently of the utility grid [3]. It should be noted that the benefits of RES-based microgrids are not only environmental but also financial. Reducing peak loads, increasing the reliability of the power supply, and improving power quality are among the auxiliary services that can be offered to the power grid operator. There is also the possibility of participation in the different electricity and ancillary services markets [4], [5]. Even though the RES offer numerous advantages, the disadvantage is that their production is variable intermittent, i.e. it cannot be perfectly predicted. This leads to the uncertainties in generation and often requires an integration of additional energy storage into the microgrid. Typically, battery storage is used to balance the difference between RES production and load demand [6]. It also offers economic benefits by reducing the need to draw the energy from the utility grid when energy prices are high, as it can be charged when the prices are low. Satisfying the load demand of the microgrid, especially in the islanded mode, depends heavily on the availability of power sources and energy storage [7]. When a situation arises that the production of RES is low and battery storage is not available or appropriate for a specific application, alternative power sources should be incorporated [8]. This power source should ideally meet two requirements: i) it should not emit any greenhouse gas emissions and ii) it should not depend on natural forces to produce the electricity. The fuel cell, which uses green hydrogen as a fuel, offers these advantages. The by-product of the reaction of hydrogen with the oxidant is water, so the environmental impact of its operation is low [9]. In addition, hydrogen can be stored in tanks and used when needed. Therefore, fuel cells are a flexible and clean power source that increases the reliability of the electricity generation [10].

The control system is responsible for maintaining the operation of a microgrid when disturbances occur, either on the generation or the load side. These disturbances include load or generation changes or switching from the grid-connected to the islanded mode of operation and vice versa. However, when faults occur, the control system is often unable to respond properly and the protection system must be activated to avoid hazards. Many papers address the problem of microgrid protection, as protecting these systems is more challenging than protecting the conventional power grid due to bidirectional power flows, varying fault current, etc. [11]. The observed microgrids typically include RES and battery storage, which contribute to the fault in different ways [12]. Although incorporating fuel cells in microgrids helps mitigating certain problems, the analysis of fuel cell response to faults is not sufficiently addressed in the literature. As one of only few relevant papers, [13] analyzes the response of a grid-connected fuel cell to faults in the distribution grid. Single-phase and three-phase faults are analysed and fuel cells with different outputs are considered. A DC microgrid with a fuel cell is analysed under fault conditions in [14]. However, the response of the fuel cell to faults is only analysed for faults at the inverters switches. In [15], a communication-based microgrid protection is proposed. The fuel cell is one of the sources within the microgrid, but its fault contribution is not analysed in detail. In [16], a method for controlling the fuel cell in case of grid faults is proposed. Again, the focus is on the control of the fuel cell rather than the fault analysis.

Per the conducted analysis, fault response of the fuel cell within a microgrid has not been adequately addressed in the literature. To fill this gap, this paper provides a thorough analysis of a fuel cell fault response. The fuel cell is analysed in a stand-alone operation and as part of a microgrid. The main contributions of this paper are the following:

- The analysis of the fuel cell fault behaviour.
- The contribution of the fuel cell to the fault conditions within the microgrid environment.

2 Fault Analysis in DC Microgrid

Failure of insulation between the two DC poles results in a pole-to-pole (PP) fault. On the other hand, pole-to-ground (PG) fault occurs when one or both conductors are connected to the ground. The PP faults are considered to be more dangerous, while the PG faults are more common and more difficult to detect [17]. The additional challenge with regard to DC microgrid protection is the lack of zero-crossing points [18]. The fault response in the time domain can be divided into two parts: the transient and the steady state. The transient part during PP faults is divided in two stages: DC-Link Capacitor Discharging Stage and Diode Freewheel Stage as is shown in Figure 1 [19]. During PG faults, there is the same DC-Link Capacitor Discharging Stage as during PP faults, except for the Diode Freewheel Stage. The fault behaviour is similar for both the PP and PG faults during the DC-Link Capacitor Discharging Stage, during which DC-link capacitor starts discharging the current exponentially through line impedance. The second stage is considered as the most challenging and it occurs with a freewheeling diodes with the converter's active devices. The current flows through the diodes and as a result there is the possibility of rapid converter's diode damage. It starts when voltage reaches zero value and therefore, all protection methods need to detect fault before this stage. PG faults are not exposed to this stage because the voltage of the DC-link capacitor will not get to zero. In the steady state part of a fault, the DC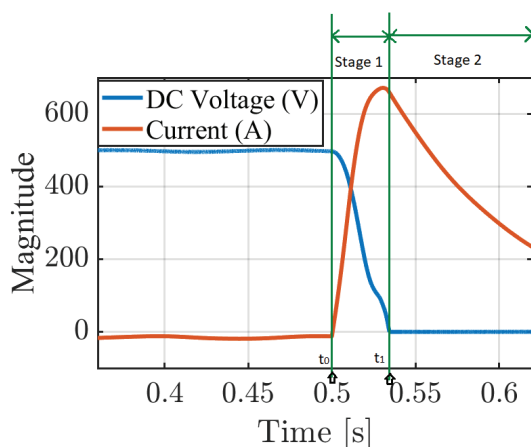 currents and voltages transition to a stable stage. The components of a microgrid contribute to the fault in different time windows. For example, discharge of the DC-link capacitor and the power converters result in current injection during transient,

Fig. 1: Pole-to-pole fault response during transient part

and RES contributes to the fault current during steady state [17].

3 System description

Figure 2 shows the DC microgrid model with corresponding connection to the AC grid through a grid-following Voltage Source Converter (VSC). The main purpose of the VSC is to regulate active and reactive power exchange with the system. The control of VSC is described using the *dq* reference frame as it is broadly applied in three-phase systems. The measured currents and voltages at the AC side are required, which are then converted using the Park transformation from a three-phase (*abc*) signal to a *dq0* synchronous frame. The microgrid is modelled using MATLAB/Simulink software. It consists of a battery energy storage system (BESS), a DC bus, a constant impedance DC load (2.5 kW), a half bridge voltage balancer [20], a fuel cell (FC), a photovoltaic (PV) system and a VSC. The PV system is considered in this study due to its popularity, while the proton-exchange membrane fuel cell (PEMFC) is considered due to its potential use in the microgrid environment. The output voltage of the common DC bus on which are parallel connected PV system, PEMFC stack, BESS, load and AC grid through power electronic converters is set to 500 V. The DC distribution lines are represented by the π-type model of a line, with the line capacitance ignored, as it is generally much smaller than the capacitance of a DC link. There are three types of grounding systems for DC microgrids: isolated grounding, one-pole grounding and mid-point grounding. Isolated grounding is avoided because it can be dangerous for humans and equipment. In this paper, the mid-point grounding with half-bridge voltage balancer is chosen because of its practical implementation. It provides a bipolar bus structure with different voltage levels (+250 V, -250 V and 500 V), thus improving the reliability of the system.

3.1 Fuel cell

The fuel cell can be considered a low-voltage source. The voltage of a single fuel cell is about 0.6 V under nominal conditions. This low voltage is insufficient for real-world applications and therefore fuel cells are stacked to achieve higher voltages. In this paper, the model of a 6 kW PEMFC stack is taken from the Matlab/Simulink library. The model consists of 65 cells with nominal efficiency of 55%. The other fuel cell parameters are listed in Table 1, together with the supply parameters.

The converter is used to achieve the desired voltage levels [21]. In this paper, the connection of the PEMFC stack is connected to the DC bus via a DC-DC boost converter. The boost converter chosen has an inductance of 0.45 mH and a capacitance of 9 mF. The used switch is a insulated gate bipolar transistor (IGBT) and a diode connected in parallel. The control of the converter ensures a constant output current.

3.2 PV system

The PV array is also taken from the built-in model library in the MATLAB/Simulink software. The chosen model consists of 4 parallel and 6 series connected strings. The irradiation is set to 1000 W/m² and temperature to 25 °C. Since the voltage of the
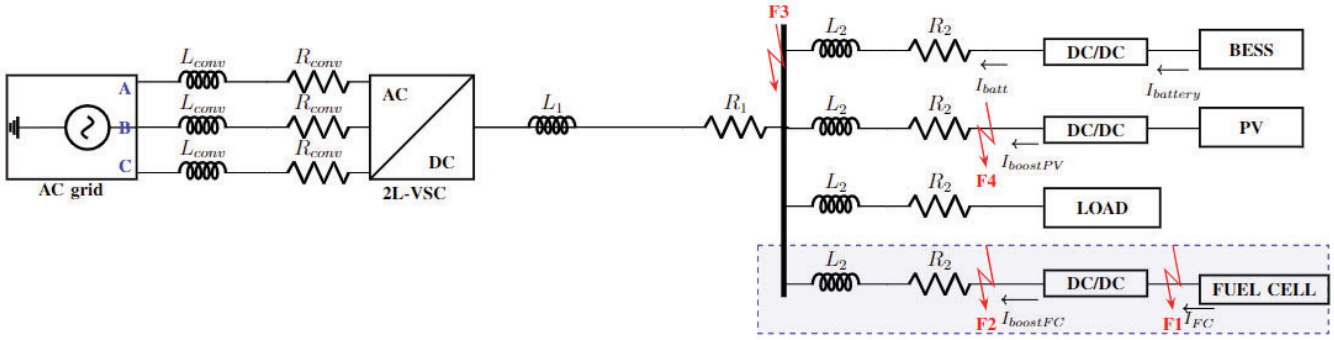
2

Fig. 2: DC microgrid with possible fault locations

Table 1 Fuel cell parameters

Voltage at 0A	65 V
Nominal operating point	133.3 A, 45 V
Maximum operating point	225 A, 37 V
Number of cells	65
Nominal stack efficiency	55 %
Operating temperature	65 °C
Nominal Air flow rate	300 lpm
Nominal supply pressure [Fuel, Air]	[1.5, 1] bar
Nominal composition [H2 O2 H2O(Air)]	[99.95, 21, 1] %

PV array is lower than the bus voltage, it is connected thorough a DC-DC boost converter. The converter inductance is 37.5 mH and capacitance is 10 mF. Maximum power point tracking (MPPT) control algorithm is used to achieve the maximum contribution from the PV array. The PV voltage and current are inputs for the MPPT control, and the output is the voltage corresponding to the maximum power of the PV [22]. The switching frequency of the pulse-width modulation (PWM) is fixed to 25 kHz to avoid high-frequency parasitic elements and noise, but also to reduce the ripple of the output voltage. The PV system can be considered as a voltage controlled current source in analysis.

3.3 BESS system

The battery energy storage system is a 12 kWh lithium-ion battery. Its nominal voltage is 120 V and the initial state of charge is 80%. A bidirectional boost converter is used to charge and discharge the battery. The parameters of the converter are as follows: inductance 2.25 mH, input capacitance 9 mF and output capacitance 10 mF. The main purpose of the BESS is to maintain the voltage of the microgrid bus at a constant value. It is performed by controlling the discharging or charging process of the battery induced by a feedback voltage busbar signal.

4 Results

Two types of faults are simulated, PP and PG, at different locations. The first objective is to provide an insight into the fault response of a stand-alone FC system. These results and simulations can help clarify the fault response when only a FC unit is available due to maintenance on other units or adverse weather conditions. The second objective is to investigate the fault behavior of the microgrid system, which includes a PV, a FC system and a BESS with corresponding converters. Transient

behaviour of a DC microgrid with RES is a key for selection of a suitable protection. Furthermore, this analysis enables a reliable and accurate fault management and protection design for DC microgrids.

4.1 Fuel Cell Unit Only

The stand-alone fuel cell fault response test is performed by short-circuiting poles of the converter output to produce a PP fault. The fuel cell is first operated under nominal conditions with a resistive load connected. Then a solid fault and a fault with a resistance of 1 Ω occur at $t = 2$s. The simulation results are presented in Figure 3. The RLC parameters of the boost converter connected to the PEMFC, the DC filter capacitor at the output of the fuel cell converter and the equivalent load all have impact on the transient response. In addition, the fault resistance has a significant effect on the transient response and the magnitude of the fault current. During the solid fault, the voltage dropped to zero because of the diode freewheeling stage, while during the resistive fault, the fall in the DC voltage is mitigated, as presented in Figure 3b. Consequently, there is a lower transient magnitude of the output DC bus current and a lower increase of the current in the FC stack during a resistive fault.

4.2 Pole-to-pole Faults

The PP faults are also named low-impedance faults and they present the largest challenge for the system. The solid PP faults are simulated at 0.5 s and are occured in the middle of the line. During the faults, breakers would not operate.

Figure 4 show the fault response for PP fault occurred between the PEMFC stack and the belonging DC-DC boost converter. The main contribution to the fault current has the FC stack current. The other sources have slight decrease in the magnitude and the summation of these fault currents at the DC bus side will be reversed. Therefore the fault current is the equal to the summation of FC stack fault current and DC bus fault current. The voltage of FC stack drops to zero while the DC bus voltage will be influenced in a short transient period (0.08s).

Figure 5 presents the fault response of the FC system terminal after the converter. Generally, the faults at unit terminals F2 or F4 can be considered as fault F3 at the DC busbar with included resistance and inductance of the distribution line. The first stage of the fault, considered as a high-rise discharging
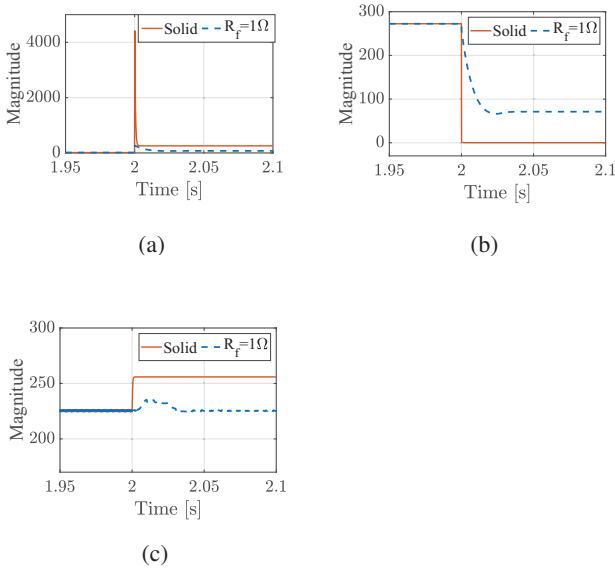
3

(a)

(b)

(c)

Fig. 3: The fault responses of stand-alone fuel cell for solid and resistive faults ($R_f=1\Omega$): (a) The converter output fault current, (b) The DC voltage, (c) The PEMFC stack current

of the DC link capacitor, will contribute a transient state of the fault current which peak starts dropping after about 3.4 ms. The contribution from the BESS is around 677 A, while the PV and FC units have the maximum reached transient fault current of around 822 A and 1566 A, respectively.

Increase in the time constant of the fault current supplied from the PV and the BESS is the result of an additional inductance of the distribution line because the inductance prevents the fast change in the current. The second stage of the fault starts after the capacitor discharging stage, when the DC voltage reaches a negative value, in this case at 0.534 s. In addition, the voltages of each source drop to zero but at the different time, depending on the time constant.

The same conclusion can be drawn for F4 fault at the PV unit, shown in Figure 7.

The PP fault F3 at the DC busbar is presented in Figure 6. The voltage falls to zero value and the contribution of each source is similar as for fault F2. The only difference is that the distribution line with the corresponding inductance and resistance decreases the fault current supplied from other sources during faults F2 and F4 at the unit terminals. The maximum transient fault contribution of the BESS, the FC and the PV systems are 891 A, 1126 A and 1210 A, while the attained steady-state fault currents are 120 A, 250 A and 35 A, respectively.

Generally, the magnitude of the peak current during PP faults becomes hundreds time higher than the rated current, depending on the internal resistance of the DC filter capacitor, capacitor value and line impedance from the capacitor source to the fault location [23]. Due to a higher time constant, fault detection should be done within a few milliseconds and before starting the second stage, and therefore it is obvious that the traditional, directional fault detection method is not be appropriate for fast fault detection.
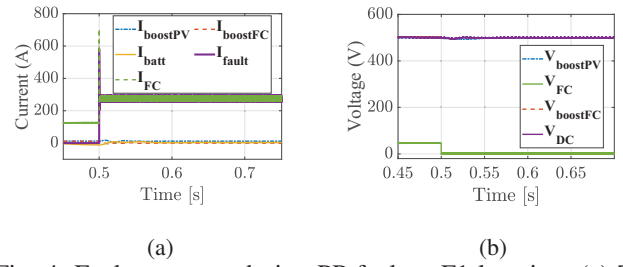

(a)

(b)

Fig. 4: Fault response during PP fault at F1 location: (a) The current contribution of the PV boost, the BESS, the FC boost, the FC stack and the fault current (b) Voltage contribution of the PV boost, the FC boost, the FC stack and the grid voltage
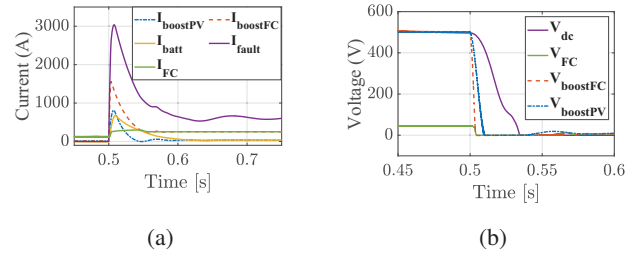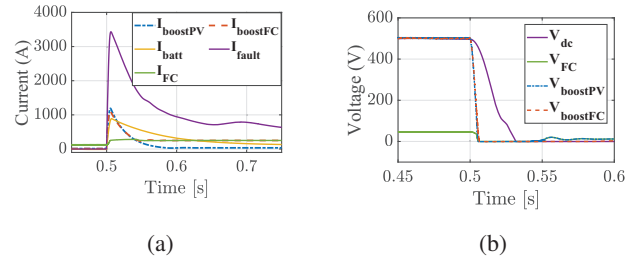

(a)

(b)

Fig. 5: Fault response during PP fault at F2 location: (a) Current contribution of the PV boost, the BESS, the FC boost, the FC stack and the fault current (b) Voltage contribution of the PV boost, the FC boost, the FC stack and the grid voltage

(a)

(b)

Fig. 6: Fault response during PP fault at F3 location: (a) Current contribution of the PV boost, the BESS, the FC boost, the FC stack and the fault current (b) Voltage contribution of the PV boost, the FC boost, the FC stack and the grid voltage

4.3 Pole-to-ground Faults

PG faults are also known as high-impedance faults. To simulate them, the positive line is connected to the ground thorough fault resistance of 3 Ω. PG faults are simulated at the same locations as the PP faults. The results of the simulations are given in Figures 8–11.

The type of grounding of the DC microgrid has an important effect on the PG fault response [24]. In addition, the half-bridge voltage balancer and its inductor have an impact on the time constant of the fault response as they are part of the fault path [22]. As the fault resistance increases, the time taken for the voltage to reach its final value also increases.

Figure 8 shows the fault between the FC and its converter. The bus voltage is affected by this fault, but it manages to restore the reference value in less than 0.2 s after the fault
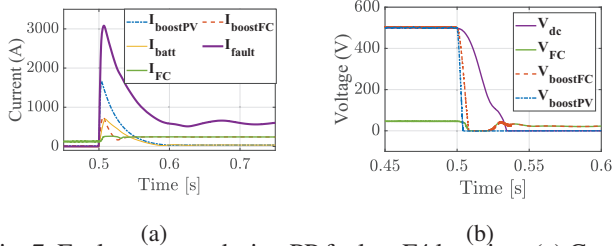
4

Fig. 7: Fault response during PP fault at F4 location: (a) Current contribution of the PV boost, the BESS, the FC boost, the FC stack and the fault current (b) Voltage contribution of the PV boost, the FC boost, the FC stack and the grid voltage

Fig. 9: Fault response during PG fault at location F2: (a) Current contribution of the PV boost, the BESS, the FC boost, the FC stack and the fault current (b) Voltage of the PV boost, the FC boost, the FC stack and the grid voltage

occurs. Voltage of the fuel cell stack is only insignificantly affected, but the current drop is considerable until the converter manages to restore the current reference value, as it operates in the constant-current mode. The currents of the BESS and the PV system are also affected by this disturbance, although not significantly.

Figure 9 shows the fault at the output of the fuel cell converter. Now the impact on the bus voltage is severe and the controller does not manage to restore the reference voltage even after 0.4 s. In contrast to the last case, the current of the fuel cell stack now increases and becomes unstable until a steady state is reached. Currents of other sources follow the same trend. Longer time constant can be seen especially at the FC stack fault current, which arises from including the voltage balancer and its inductor in the fault impedance. In this case, a steady state fault current is reached after about 1.5 s, as compared to 0.08 s in case of pole to pole fault.

Figures 10 and 11 show the response for the fault at locations F3 and F4. The fault responses correspond to the fault response of the fault at location F2, however, the magnitudes of the currents are changed. The resistance of the line between the fault and the power source reduces the fault current magnitude. As it can be seen, the current peak value depends on the fault path.

Comparing PG to PP faults, we find that PG faults cause lower magnitude fault currents and voltage drops. The contribution of the FC and PV systems is not as large as in the PP faults case, and is therefore more difficult to detect. Compared to the PP faults, oscillations of PG fault currents are more obvious. Furthermore, PG faults are not as devastating to power
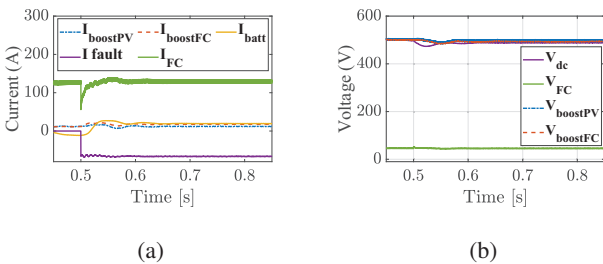

Fig. 10: Fault response during PG fault at location F3: (a) Current contribution of the PV boost, the BESS, the FC boost, the FC stack and the fault current (b) Voltage of the PV boost, the FC boost, the FC stack and the grid voltage
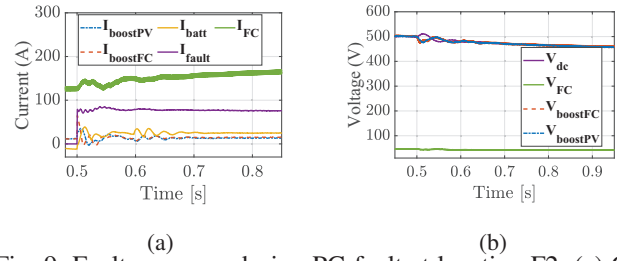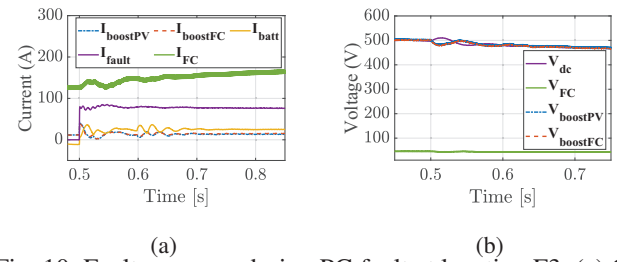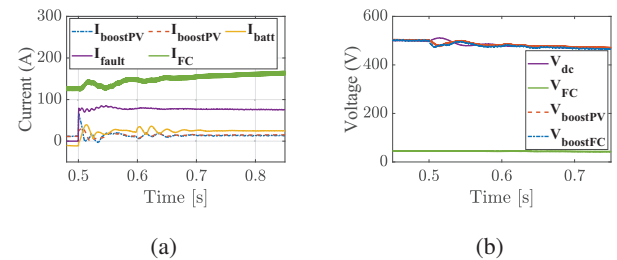

Fig. 11: Fault response during PG fault at location F4: (a) Current contribution of the PV boost, the BESS, the FC boost, the FC stack and the fault current (b) Voltage of the PV boost, the FC boost, the FC stack and the grid voltage

converts as PP faults because of the lack of the diode freewheel stage.

5 Conclusion

This paper analyses in detail the fault response of the PEMFC system, both as a single unit and as a part of a RES-based DC microgrid. The analysis focuses on both the PG and PP faults and forms the basis for the development of a suitable protection system. The model presented can also be used to simulate different types of faults at various locations in order to develop and test suitable protection for a fuel cell or an entire microgrid. The limitations of the analysis performed result from operating all power sources at a fixed operating point. Future work can focus on incorporating different operating points at which the microgrid could operate. In addition, the choice of power sources and storage types that accompany the fuel cell in the

Fig. 8: Fault response during PG fault at location F1: (a) Current contribution of the PV boost, the BESS, the FC boost, the FC stack and the fault current (b) Voltage of the PV boost, the FC boost, the FC stack and the grid voltage

5

microgrid was made based on popularity in the literature, but power sources of other types can be included. For example, electrolyzers, supercapacitors, and renewable energy sources such as wind turbines can be included. The battery technology used in this work is the lithium-ion battery, but other technologies may be considered depending on the application.

6 Acknowledgement

7 References

[1] N.L. Panwar, S.C. Kaushik, Surendra Kothari, "Role of renewable energy sources in environmental protection: A review" in Renewable and Sustainable Energy Reviews, vol. 15, no. 3, pp. 1513-1524, 2011.

[2] Hrvoje Pandzic, Yury Dvorkin, Ting Qui, Yishen Wang, and Daniel Kirschen, "Toward Cost-Efficient and Reliable Unit Commitment Under Uncertainty" in IEEE Transactions on Power Systems, vol. 31, no. 2, pp. 970-982, March 2016.

[3] R. H. Lasseter and P. Paigi, "Microgrid: a conceptual solution," 2004 IEEE 35th Annual Power Electronics Specialists Conference, 2004, pp. 4285-4290 Vol.6

[4] G. Y. Morris, C. Abbey, S. Wong and G. Joós, "Evaluation of the costs and benefits of Microgrids with consideration of services beyond energy supply," 2012 IEEE Power and Energy Society General Meeting, 2012, pp. 1-9

[5] Hrvoje Basic, Tomislav Dragicevic, Hrvoje Pandzic, and Frede Blaabjerg. DC microgrids providing frequency regulation in electrical power system – imperfect communication issues, in Proceedings of 2017 IEEE Second International Conference on DC Microgrids, Germany, June 27-29, 2017, pp. 434-439.

[6] Mateo Beus, Frederik Banis, Hrvoje Pandzic, and Niels Kjolstad Poulsen. Three-level hierarchical microgrid control—model development and laboratory implementation, Electric Power Systems Research, vol. 189, 106758, December, 2020.

[7] Mateo Beus, Ivan Grcic, and Hrvoje Pandzic. Microgrid Dispatch with Protection Constraints, in Proceedings of 2021 International Conference on Smart Energy Systems and Technologies, Finland, September 6-8, 2021, pp. 1-6.

[8] A. Naeem and N. U. Hassan, "Renewable Energy Intermittency Mitigation in Microgrids: State-of-the-Art and Future Prospects," 2020 4th International Conference on Green Energy and Applications, 2020, pp. 158-164

[9] Mohammad Ali Abdelkareem, Khaled Elsaid, Tabbi Wilberforce, Mohammed Kamil, Enas Taha Sayed, A. Olabi, Environmental aspects of fuel cells: A review, Science of The Total Environment, Volume 752, 2021.

[10] A. Khaligh and Z. Li, "Battery, Ultracapacitor, Fuel Cell, and Hybrid Energy Storage Systems for Electric, Hybrid Electric, Fuel Cell, and Plug-In Hybrid Electric Vehicles: State of the Art," in IEEE Transactions on Vehicular Technology, vol. 59, no. 6, pp. 2806-2814, July, 2010.

[11] Belwin J. Brearley, R. Raja Prabu, A review on issues and approaches for microgrid protection, Renewable and Sustainable Energy Reviews, vol. 67, pp. 988-997, 2017.

[12] Ivan Grcic, Hrvoje Pandzic, and Damir Novosel. Fault Detection in DC Microgrids Using Short-time Fourier Transform, Energies, vol. 14, 277, 2021.

[13] E. M. Stewart, R. Tumilty, J. Fletcher, A. Lutz, G. Ault and J. McDonald, "Analysis of a Distributed Grid-Connected Fuel Cell During Fault Conditions," in IEEE Transactions on Power Systems, vol. 25, no. 1, pp. 497-505, February, 2010.

[14] W. Lee and S. Kang, "Protection for distributed generations in the DC micro-grid," 2011 2nd IEEE PES International Conference and Exhibition on Innovative Smart Grid Technologies, 2011, pp. 1-5

[15] S. Thale and V. Agarwal, "Controller Area Network (CAN) based smart protection scheme for Solar PV, fuel cell, Ultra-Capacitor and wind energy system based microgrid," 2012 38th IEEE Photovoltaic Specialists Conference, 2012, pp. 580-585

[16] A. Mojallal and S. Lotfifard, "Improving During and Postfault Response of Fuel Cells in Symmetrical and Asymmetrical Grid Fault Cases," in IEEE Transactions on Sustainable Energy, vol. 9, no. 3, pp. 1407-1418, July 2018.

[17] Z. Ali et al, "Fault Management in DC Microgrids: A Review of Challenges, Countermeasures, and Future Research Trends," in IEEE Access, vol. 9, pp. 128032–128054, 2021.

[18] J. Skare, M. Mesic, "Protection devices and selectivity in DC power distribution sub-systems," in Journal of Energy: Energija, vol. 58, no. 1, pp. 75–97, February, 2009.

[19] Z. Zhang, Q. Chen, R. Xie, K. Sun, "The fault analysis of PV cable fault in DC microgrids," in IEEE Transactions on Energy Conversion, vol. 34, no. 1, pp. 486-496, October 2018.

[20] Han, Byung-Moon, A Half-Bridge Voltage Balancer with New Controller for Bipolar DC Distribution Systems, in Energies, vol. 9, no. 3, 2016.

[21] R.A. Linares-Lamus, S. Raël, K. Berger, M. Hinaje and J. Lévêque, "PEM single fuel cell as a dedicated power source for superconducting coils," in 9th International Exergy, Energy and Environment Symposium , Split, Croatia, May, 2017, pp. 415-421

[22] E.W. Nahas, H.A. Abd el-Ghany, D.E.A. Mansour and M.M. Eissa, "Extensive analysis of fault response and extracting fault features for DC microgrids," in Alexandria Engineering Journal, vol. 60, no. 2, pp. 2405-2420, April 2021.

[23] S. Beheshtaein, R. M. Cuzner, M. Forouzesh, M. Savaghebi, and J. M. Guerrero, "DC microgrid protection: A comprehensive review," in IEEE Trans. Emerg. Sel. Topics Power Electron, March, 2019.

[24] J. Mohammadi, F. B. Ajaei, and G. Stevens, "Grounding the DC microgrid," in IEEE Transactions on Industry Applications, vol. 55, no. 5, pp. 4490–4499, July, 2019.